Equatorial cavities on asteroids, an evidence of fission events

Simon Tardivel[a], Paul Sánchez[a], Daniel J. Scheeres[b]

[a] *Colorado Center for Astrodynamics Research, The University of Colorado Boulder*
UCB 431, Boulder, CO 80309-0431
simon.tardivel@colorado.edu
[b] *Department of Aerospace Engineering Sciences, The University of Colorado Boulder*
UCB 431, Boulder, CO 80309-0431

Abstract

This paper investigates the equatorial cavities found on asteroids 2008 EV5 and 2000 DP107 Alpha. As the likelihood of these cavities being impact craters is demonstrated to be low, the paper presents a fission mechanism that explains their existence as a scar of past fission events. The dynamical environment of bicone (or "top"-shaped) asteroids is such that, at high spin rates, an identifiable equatorial region enters into tension before the rest of the body. We propose hypothetical past shapes for 2008 EV5 and 2000 DP107, with mass added within the cavity to recreate a smoother equatorial ridge. The dynamical environment of these hypothetical parent bodies reveal that this modified region is indeed set in tension when spin is increased. The fission process requires tensile strength at the interface between the ejecta and the remaining body, at the moment of fission, between 0 to 2 Pa for 2008 EV5 and between 0 to 15 Pa for 2000 DP107, depending on the precise fission scenario considered. Going back to the spin-up deformation phase of the asteroids, the paper examines how kinetic sieving can form predominantly rocky equators, whose tensile strength could be much lower than that of the rest of the body. This process could explain the low cohesion values implied for this fission mechanism.

Keywords: asteroid; fission; effective gravity; structure; cohesion

1. Introduction

Until very recently, the small bodies of the Solar System were only sparkling dots moving in front of a background of stars in the lens of a telescope. But with the advent of small body exploration missions (e.g. NEAR-Shoemaker[1], Hayabusa[2, 3], Rosetta[4]) and radar imaging, we know they come in many shapes and forms. And yet, some patterns have started to emerge, notably the biconic asteroid.

A bicone can be defined as the joining of two cones by their base. This joining create an axisymmetric shape with an equatorial ridge; it also gives the asteroid a very identifiable diamond profile. Also referred to as a "spinning-top" shape, many asteroids seem to adopt this shape, particularly when their spin rate is fast such as single asteroids 2008 EV5 and Bennu. Some others even have such a high spin that it brings their equator to the limit of break-up, e.g. 1999 KW4 Alpha, 1996 FG3 Alpha and DP107 Alpha.

Contrary to large planetary bodies, the shape of an asteroid is not due only to their gravity and spin rate. It is due in a large part to the structure of the asteroid itself and the properties of its constitutive material. Large monoliths and volumes of fine grains do not exhibit the same behavior and do not conduce to the same physical arrangements. The structure of small bodies has therefore become a major topic for planetology. Beyond the scientific understanding it brings, asteroid structure is a major question should it be necessary to deflect an asteroid set on a collision course with the Earth. Understanding the effect that a high-velocity deflection impactor could have on an asteroid requires knowledge of what lies beneath the surface of the asteroid. However, probing an asteroid's inner structure is a difficult task, which requires sounding technologies either from an orbiter or from a lander. But this structure and more generally the sort of material we can expect to find on an asteroid leaves many clues: one such clue is the shape itself and especially odd or unusual features.

This paper investigates the equatorial cavities found on asteroids 2008 EV5 [5] and 2000 DP107 Alpha [6]. These two asteroids are of the bicone type mentioned and present large cavities. Our interest in these cavities is twofold. First, there is no clear explanation for their existence. Second, we know binary formation may be caused by fission [7, 8] at high spin rates acquired from Yarkovsky-O'Keefe-Radzievskii-Paddack (YORP) effect [9], but the mechanism through which this formation occurs is not well understood. Is it possible that binary formation and cavities are both the byproduct of

fission? Here, we argue that the equatorial cavities found on fast rotators could be evidence of a binary formation mechanism and, more generally, provide some insight into the structure of both primary and secondary of binary systems..

The outline of the paper is as follows. Section 2 will present and discuss in more details the equatorial cavities of 2008 EV5 and 2000 DP107 Alpha. This discussion leads to the conclusion that these cavities were most probably created by the dynamics of these asteroids, and we propose a fission hypothesis. To understand the possibility of fission, section 3 examines the dynamical environment of a fast spinning asteroid. We notably define the surface delimiting regions of the asteroid feeling an outward pull from the rest of asteroid when the spin rate is high enough, and that we name the h^* surface. In general, this surface singles out only one region, despite the apparent axisymmetry of the considered bodies. Section 4 puts this understanding into use and observes what happens to the h^* surface when the equatorial cavities are filled with mass. We conclude that this fission mechanism may very well be the cause of the cavities of 2008 EV5 and 2000 DP107 Alpha and we discuss the characteristics of this fission event and of the ejecta. Yet, this mechanism requires a very low tensile strength of the equatorial material of the bodies. Therefore, we go back to the structure of such bicone asteroids. Investigating how they may have formed, we explain why such tensile strength is coherent with the history of these asteroids, as hinted at by their bicone shape.

2. Equatorial cavities

2008 EV5 is a ≈450 m equatorial diameter asteroid. 2000 DP107 is a binary asteroid system, where the primary (largest) body, named Alpha, has an equatorial diameter of ≈950 m. Both are NEOs. But their interest, for this specific study, is that they display a puzzling feature: a large, deep cavity located at the equator.

2.1. Equatorial cavities

The shapes of 2008 EV5 and 2000 DP107 Alpha were revealed when radar imaging was obtained [5, 6]. Like many other asteroids in the 0.2-2 km range, EV5 and DP107 present a bicone profile around their pole. This shape is thought to be acquired through deformation of the body under fast spin rates [10] – the paper goes back to and expands this discussion in its last section. Eventually, the fast spin rate creates an equatorial ridge that clearly delimits the two cones that form the two hemispheres of the body.

The resolution of the radar imaging and associated shape models is sufficient to establish the existence of anomalies located at the eaquator for both EV5 and DP107. These anomalies are cavities in the otherwise smooth equatorial ridge present on the two bodies. The shape of EV5 can be seen in figure 1 and the shape of DP107 in figure 2. Though the process of creation of a bicone shape asteroids is progressively becoming understood, such a process does not readily provide an explanation for the presence of a cavity at the equator. To the best of our knowledge, the creation process of a large cavity has never been successfully simulated (or observed). The very presence of an equatorial cavity is then unexplained, and begs the question of the mechanisms that could have created one.

We also note here that other asteroids have surface structures similar to these cavities. For instance, the high latitudes and poles of 1999 KW4 Alpha or of 1996 FG3, present depressions. The asteroid 2002 CE26 has asymmetric hemispheres, with a southern hemisphere very rich in flats, depressions and protrusions[11]. However, these examples do not exhibit the clear equatorial cavity identified for 2008 EV5 and DP107 Alpha and are therefore not included in our analysis.

Table 1 presents the characteristics of the two asteroids considered here. The diameter noted here is the average equatorial diameter. The density was fixed for both bodies at 1.3 g/cm^3 to allow for mutual comparison – their actual densities probably differs, with estimations for 2000 DP 107 of 1.381

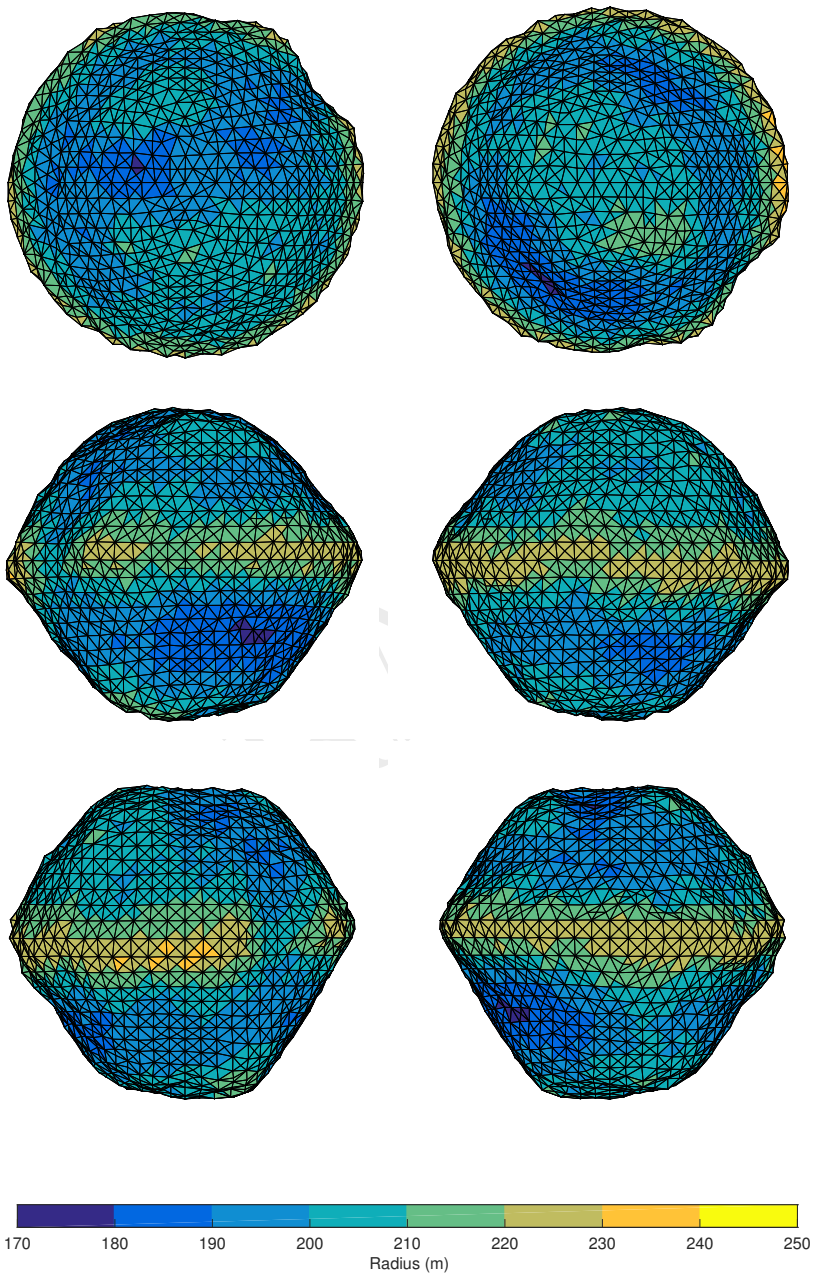

Figure 1: View of 2008 EV5 [5] in its present shape, viewed from $+\hat{z}$ (top left), $-\hat{z}$ (top right), $+\hat{y}$ (mid left), $-\hat{y}$ (mid right), $+\hat{x}$ (bottom left), $-\hat{x}$ (bottom right). The surface is colored along the facet's distance to the center of the body.

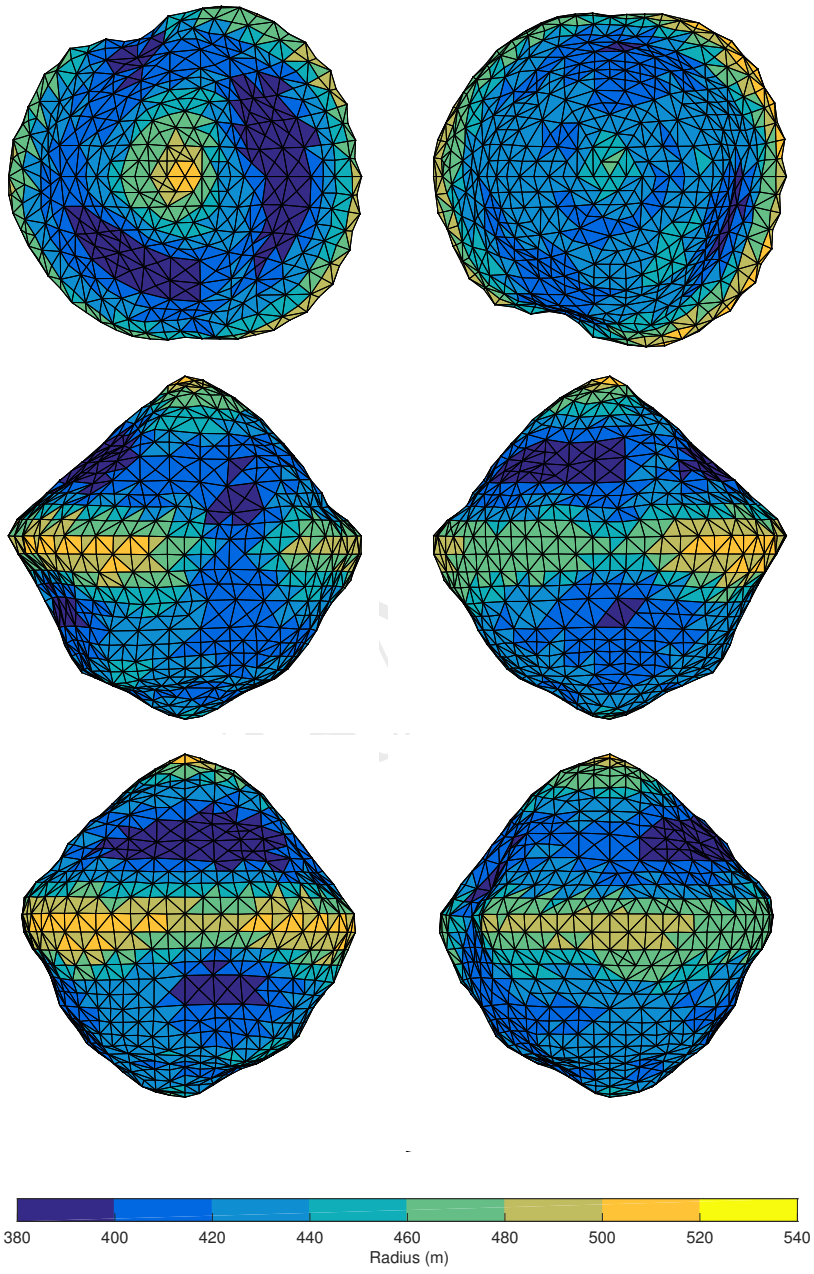

Figure 2: View of 2000 DP107 Alpha [6] in its present shape, viewed from $+\hat{z}$ (top left), $-\hat{z}$ (top right), $+\hat{y}$ (mid left), $-\hat{y}$ (mid right), $+\hat{x}$ (bottom left), $-\hat{x}$ (bottom right). The surface is colored along the facet's distance to the center of the body.

$\pm$ 344 g/cm^3 while the density of 2008 EV5 is not well constrained. The size of the cavity is approximate and is computed by measuring the length of the arc from the two highest points found on each side of the cavity at the equator, rounded to the nearest 10m.

Table 1: Parameters for the considered asteroids.

Body	Diameter (m)	Density (g/cm^3)	Cavity diameter (m)	Cavity depth (m)
2008 EV5	$\approx$450	1.3	$\approx$160	$\approx$20
2000 DP107 Alpha	$\approx$950	1.3	$\approx$400	$\approx$60

2.2. The crater hypothesis

In the very paper that established the existence of the cavity of EV5, a hypothesis was made on the mechanism that formed this cavity. It was hypothesized by Busch et al. that the cavity could be a crater, or a resurfaced crater, caused by the high-velocity impact of a much smaller asteroid. This explanation is possible but unlikely.

Before considering the chance of such an impact occurring, it has to be noted that such explanation requires, per se, an alignment of conditions: 1. such impacts must be frequent enough that they occurred for at least two of our shape-resolved asteroid, 2. such impacts must be rare enough that they were not observed on more asteroids or more often on a same asteroid. This combination, in itself, already constrains the crater hypothesis. These impact events must have a timestamp equal or inferior to the scale of approximately 1 million years: YORP effects are thought to cause resurfacing of a body within such a time frame [9].

Consider the example of EV5. We have measured a 165 m cavity, hence a 165 m hypothetical crater. The impactor needed to create such a crater would be 10 to 30 times smaller, depending on its speed and composition but also the type of material response expected from EV5. Using Nolan et al.[12], and accounting for faster collision speeds for NEOs than for main belt asteroid, we have that a 165 m crater would be formed by a 3.5m diameter impactor. Using Bottke et al.[13] we obtain the current number N of projectiles of such a size (or larger) in the NEO population: N is approximately 1 billion. We then assume an intrinsic collision probability P of 3×10^{-18} km^{-2}yr^{-1} from Bottke et al.[14]. The number of such impact events per year is then given by:

(1)

The 200 m diameter cavity would correspond to a minimum 100 m radius impact crater. Such a crater would be created by a projectile of minimum diameter of 5 m. Using Bottke et al. [13, 14], the chance of such a collision occurring on a NEO and in a timespan less than 1 My is approximately 1 in 60,000. Thus, with less than 60 asteroids that have their shape resolved as of today, the chance of observing a single one of these craters, in this population, should be less than 1 in 1,000. The chance of observing two of these craters is less than 1 in a million.

This calculation does not even consider that: 1. the calculation for DP107 yields even much lower probabilities than for EV5 and 2. the impact should occur at the equator and at a high impact angle, which even further decreases the overall probability of such an impact. The crater hypothesis is therefore invalid to a degree of certainty of at least 4.5σ, with the most generous of assumptions.

2.3. Evidence of fission

If the cavity does not form through exterior causes, it must then be linked to the asteroid itself. Since these bodies are not comets, some sort of solar activity (causing extensive and periodic resurfacing) cannot be responsible. We are then left with finding a dynamical cause to the cavity. And to the point, the equator of a fast spinning asteroid is a dynamically significant region. Yet, the equator is a region where mass tends to flows to, not where mass recedes from [15, 10] – as an example of this point, planetary bodies all exhibit some flatness. Hence it is difficult to explain how a cavity can form naturally through the deformation of the system. In finite element simulations, the deformation of bodies through spin has never been observed, to the best of our knowledge, to create equatorial cavities.

In this paper, we present a mechanism that can explain the formation of these cavities: fission. We postulate that an original EV5 or DP107 did not present such a cavity, but it underwent fission at a high spin rate. Then an ejecta, representing a small portion of the asteroid (1-10% in mass), was created. In the case of 2000 DP107, the ejecta or part thereof became the secondary body of the presently stable binary system. In the case of 2008 EV5, as no secondary seems to be present the ejecta could have spiraled out of the main body's influence or redeposited near the equator, in full or in part.

This mechanism is of interest for two reasons. First, as mentioned, it is a plausible explanation to the presence of an observed equatorial cavity on two fast rotators. But, more importantly, it is a fission mechanism that allows for the formation of a binary system. Fission through YORP spin-up has already been established as the source of most binary systems [8], but the mechanism through which the fission takes place has not been identified. Indeed, the only observed small body fission was a catastrophic disruption [16, 17]. In the fission mechanism considered here, and echoing the formation process described by Sánchez and Scheeres [18], a whole chunk of the asteroid is ejected at once. Its tight initial orbit leads to many possible outcomes: impact, ejection, regularization, disruption, etc. At the moment of fission, the event leaves a clear mark – an equatorial cavity – on the parent body. However resurfacing can eventually, over time, hide the scar. The rest of the paper will present evidence and rationale for this fission mechanism.

2.4. Filling the cavity

Before examining the specific mechanism of fission in the next section, we need to reconstitute what the original body could have looked like. We have no definite information on this original body, so we make some assumptions of parsimony: 1. The original asteroid was only different from the actual at the cavity region; 2. The local shape at the cavity was comparable to that of the rest of the body; 3. The mass in the cavity was of the same density as the rest of the body.

However, we leave ourselves one important parameter that we can alter: the maximum height d, above the projected equatorial level, of the mass that we put instead of the cavity. When this added mass height is of 0 m, it means that the mass simply filled the cavity, and it locally reaches the level of the equator that is measured on each side of the cavity. But we also considered the possibility that the mass placed there could protrude slightly from the average equatorial level. This idea comes from our observation of fission mechanisms in discrete-element simulation: it generally shows that partial fission is preceded by a non-axisymmetric deformation, creating a protrusion on one side of the asteroid [18]. We limit our study cases to small protrusions, not exceeding 30% of the radius of the body and limited to the cavity region.

The way we recreate the asteroid is by inflating it, i.e. by pulling outwards the vertices located within the cavity. We define an ellipse in longitude latitude, centered on the cavity. The contour of this ellipse defines the reference

shape, while a point within the ellipse is altered solely through a modification of its radius r, keeping identical longitude and latitude. Each inner point is matched with two contour points, located on the contour of the ellipse at the same (approximately) latitude and on both sides, east and west, of the inner point. These two contour points P_1 and P_2 act as shape references for the inner point.

The new radius of the inner point can be then written as $r = m+\delta$. Here, m represents the value of the radius if it was simply computed as a linear transition between the two contour points (east and west). δ is the deformation term. To make the shape smooth and realistic, both m and δ depend on the inner point longitude relative to the center of the cavity/protrusion. Denoting l the longitude of the inner point, l_0 the longitude of the center of the cavity, and l_1, r_1, l_2, r_2 the longitude and radius of its corresponding contour points:

$$m = (r_1 - r_2)\frac{l_2 - l}{l_2 - l_1} + r_2 \tag{2}$$

The computation of δ is more complex. To parametrize the shape of the protrusion in order to better reflect real examples and finite element simulations, δ is broken up as: $\delta = d\,\lambda_{\text{lon}}\,\lambda_{\text{lat}}$. d is the additional height above the equatorial level. λ_{lon} and λ_{lat} are functions of, respectively, the relative longitude and the relative latitude, both normalized. The normalized relative longitude is $|1 - (l_0 - l)/\Delta l|$ where Δl is the maximum longitudinal extent of the cavity, the normalized relative latitude is defined similarly. We represent their profile along, respectively, longitude and latitude, on fig. 3. Each λ function is a piecewise-defined, continuous assembly of two second order polynomials. Both functions have value 0 at the edge of the cavity and 1 at the center of the cavity, and 0 first derivative there as well. The two polynomials meet at (0.5,0.5) for λ_{lon} and at (0.75,0.5) for λ_{lat}.

It must be noted that the process of filling the cavity, as well as adding the protrusion, increases the total mass of the body. The added mass depends on the additional height d, but also on the specific profiles of λ_{lon} and λ_{lat}. The difference can be quite important, and it impacts the fission mechanism results. Since the modified asteroid present no cavity anymore, we talk about the "protrusion region" when discussing this modified location. A last step must be taken after the protrusion is created: this additional mass has offset the center of mass of the asteroid. Keeping the shape as is would create a non-physical potential field. The simplest way to correct for this misalignment is to move the whole shape, so that the new center of mass coincides again

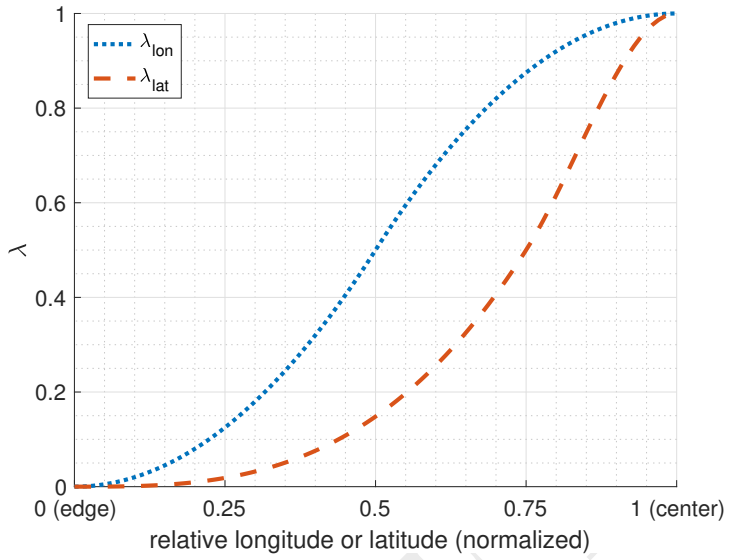

Figure 3: The protrusion is shaped using the functions λ_{lon} and λ_{lat}

with the origin of the frame.

Different cases were envisaged for each body. For 2008 EV5, we considered 5 cases: 0 m (filled cavity) 15 m, 30 m, 45 m and 60 m protrusion height. For 2000 DP107, we considered 5 cases as well: 0 m (filled cavity), 30 m, 60 m, 90 m and 120 m protrusion height. Each case added mass to the body, and this additional mass was recorded and is used to select the fission period (see following subsection). Figure 4 presents the shapes of 2008 EV5 in its present form[5], with a filled cavity and with a 30 m protrusion. Figure 5 presents the shapes of 2000 DP107 in its present form[6], with a filled cavity and with a 60 m protrusion. Both figures give top views and side views – the top view is the canonic top view ($\hat{x}$-axis to the right, $\hat{y}$-axis to the top) whereas the side view places the cavity/protrusion to the right.

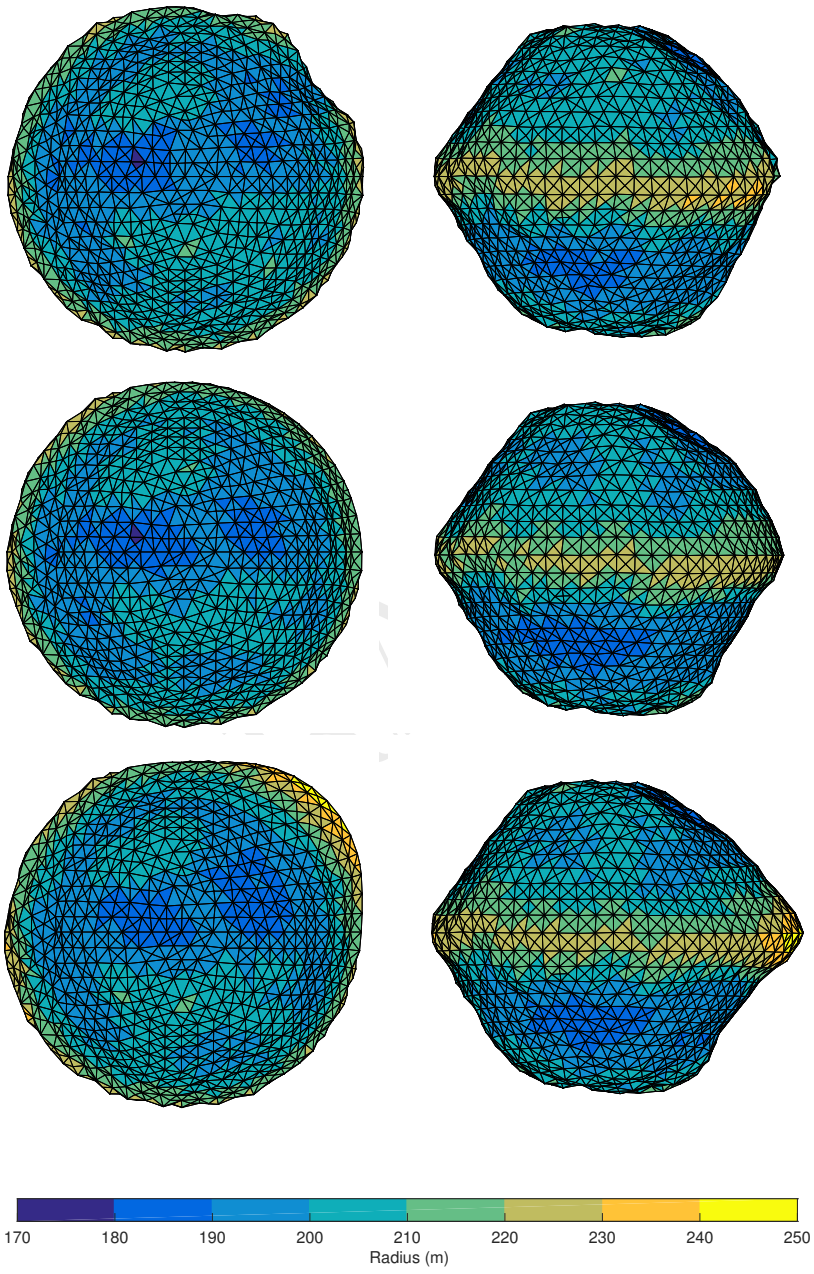

Figure 4: Top view (left) and side view (right) of 2008 EV5 in its present shape (top)[5], with a filled cavity (middle) and with a 30 m protrusion (bottom). The surface is colored along the facet's distance to the center of the body.

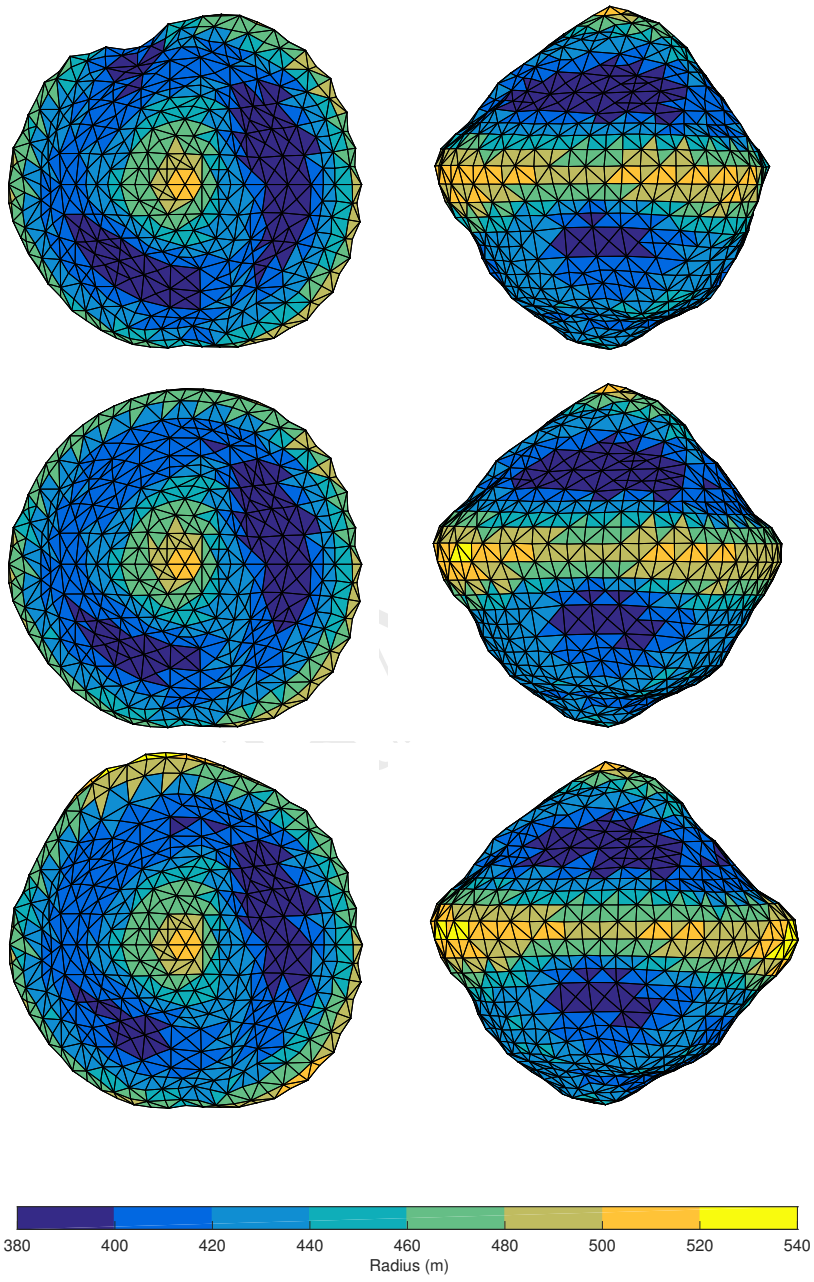

Figure 5: Top view (left) and side view (right) of 2000 DP107 in its present shape (top)[6], with a filled cavity (middle) and with a 60 m protrusion (bottom). The surface is colored along the facet's distance to the center of the body.

3. The effective gravity field of fast rotating bodies

To understand the fission of small bodies, one must examine the forces that act on a rock, or an aggregate of particles, at the surface. In this section, we examine the dynamical environment of the asteroid in its rotating frame, i.e. the combination of centrifugal and gravitational forces, to identify the necessary conditions for fission. Simply put, we wonder when a particle of a small body stops feeling a "downward" pull.

3.1. Effective potential

As aforementioned, the two main external forces acting on a rock resting at the surface of a small body, considered of homogeneous density, are the gravitational force, stemming from the mass distribution of the body, and the centrifugal force, stemming from the spin rate of the body. These two forces acting proportionally to the mass of the particle they influence, we reason simply in terms of accelerations rather than forces. The sum of these two accelerations is oft called the effective gravity as it represents the real acceleration one would feel from gravity amended from the centrifugal outward pull.

Mathematically, the gravity field is a potential field that we denote U. The effective gravity is also a potential field, which we denote Ω. The frame of reference we use assume the spin rate $\boldsymbol{\omega}$ is along the positive $\hat{z}$ axis, the other axes $\hat{x}$ and $\hat{y}$ being arbitrary. We also introduce the notation h that defines the cylindrical radius, i.e. $h = \sqrt{x^2 + y^2}$. In that frame, Ω is defined as:

$$\Omega = U - \frac{1}{2}\omega^2(x^2 + y^2) = U - \frac{1}{2}\omega^2 h^2 \tag{3}$$

The equations of motion of a moving particle in this field are:

$$\begin{cases} \ddot{x} &= -\dfrac{\partial \Omega}{\partial x} - 2\omega\dot{y} \\ \ddot{y} &= -\dfrac{\partial \Omega}{\partial y} + 2\omega\dot{x} \\ \ddot{z} &= -\dfrac{\partial \Omega}{\partial z} \end{cases} \tag{4}$$

3.2. h, zh* and the ridge line*

The previous equations are useful when integrating the motion of an orbiter or otherwise free moving particle. But, in the situation at hand, we want to determine when a rock, or an aggregate of rocks, initially at rest, might separate from the asteroid due to external forces. This moment occurs when the centrifugal acceleration overcomes the gravitational acceleration. Assuming the object rests at some distance h from the $\hat{z}$ axis, this condition can be mathematically put as:

$$\frac{\partial \Omega}{\partial h} < 0 \tag{5}$$

This condition naturally leads us to introduce the h^* surface. This surface is formally defined as the locus of points such that the total acceleration on the $\hat{\boldsymbol{h}}$ direction (horizontal or cylindrical radius) is zero. For a homogeneous sphere, h^* is composed of a sphere of radius $\sqrt[3]{\mu/\omega^2}$ (the body's geosynchronous radius) and of the $\hat{z}$ axis. For the most arbitrary of mass distributions and spin rates, the shape or even nature of h^* is quite unpredictable. Yet, under reasonable assumptions and slow spin rates, it is a single, connected 2-dimensional surface that surrounds the body and attaches to the $\hat{z}$ axis at higher latitudes [19]. In details, the structure of h^* near the $\hat{z}$ axis is quite complex, due to the fundamental degeneracy of a derivative by the cylindrical radius close to the pole singularity. Yet, as will be clear in later developments, this is a detail that does not affect the regions close to the surface and near the equator which are the focus of this paper. For all intents and purposes it can be considered that, locally, h^* is a roughly spherical shell, within which the horizontal acceleration is inward, and beyond which the horizontal acceleration is outward.

From these observations, the main purpose of h^* is to delimit regions that feel an inward pull or an outward pull. At a given spin rate, regions of a body that lie beyond the h^* surface feel outward acceleration and hence are prone to shedding. All our further results are based on the computation of $h*$ and its intersection with the body. Nevertheless, before going into the precise fission mechanism presented in this paper, we introduce two related concepts: z^*, zh^* and the ridge line.

z^* is the locus of points where the vertical (on $\hat{z}$) acceleration is zero. For (natural) small bodies, z^* is a single sheet, deformation of the xy-plane. We then refer to it as the z^* plane (following the nomenclature of differential geometry) and it consists, for each x and y, in the value of z for which Ω,

as a function of z, reaches a global minimum. The use of z^* is essentially to define a *dynamical equator* where one can conduct simplified planar studies (e.g. using zero-velocity curves). zh^* is defined as the locus of points where both radial (on $\hat{h}$) and vertical (on $\hat{z}$) acceleration are zero. For natural mass distributions such as small bodies, zh^* is essentially a near-equatorial cut of h^*.

Since h^* has a complex structure close to the $\hat{z}$ axis, zh^* inherits this structure and thus comprises two distincts features for slow enough spin rates: this inner feature close the $\hat{z}$ axis, and an outer feature that encompasses the body entirely. This latter structure is called the ridge line as it represents visually the ridge of the effective potential drawn on z^*. The interest of the ridge line is threefold; first it is a 1-dimensional representation of h^* and thus allows for an easy visualization of the evolution of h^*; second it is a perfectly well defined and well behaved (at slow spin rates), smooth curve, contrarily to the degenerate h^*; third it contains all the exterior equilibrium points of the system, which will allow further dynamical understanding of the situation. Figures 6 and 7 present h^*, z^* and zh^* in a more visual way through, respectively, a vertical cut and a z^* projection.

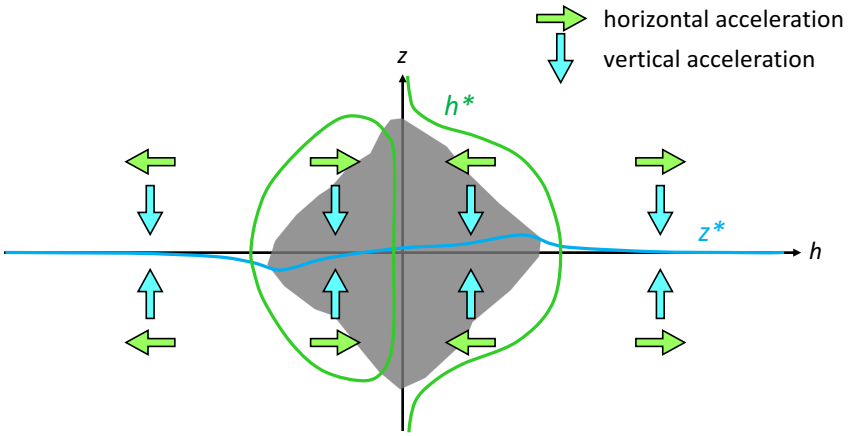

Figure 6: Vertical cut passing through the origin, showing the intersection with z^* and h^*, for a typical slow-rotating asteroid.

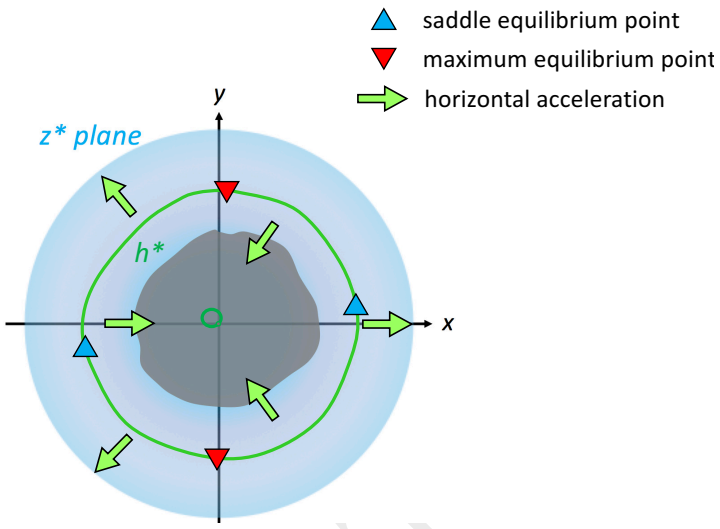

Figure 7: Top-down view showing the z^* plane and, on it, zh^* (ridge line and central degenerate structure), as well as the outer equilibrium points, for a typical slow-rotating asteroid.

3.3. Evolution during spin-up

As one may have noted, the previous definition of the ridge line was made at slow spin rate. For an extremely slow spin rate, where the body shape does not matter, the ridge line is rejected to very large distances and asymptotic to a circle of radius $\sqrt[3]{\mu/\omega^2}$, the classic geostationary radius. As the spin rate is increased, the ridge line approaches the body. For an arbitrary body, the ridge line deforms from its asymptotic circle at infinity. It eventually comes a spin rate for which the ridge line touches the surface of the body. For a perfect sphere or a perfect ellipsoid, this is the end of the journey for the ridge line as it collapses instantly to the center. But for a body of less symmetric shape, the ridge line topological structure is generally preserved and it starts diving inside the body. The evolution of the ridge line at varying spin rates was already conducted for Bennu, another bicone asteroid, in a previous work [20]. We refer the reader to this work for additional details, as well as more detailed figures (figures 19 and 20), on the aforementionned new structures on an example asteroid. We will here present the generic behavior observed for this type of asteroids.

In practice, this first intersection point is always found to be located very close to the ("saddle"-type) equilibrium point of lowest energy. As soon as this first point enters the body, it starts dipping inward much more

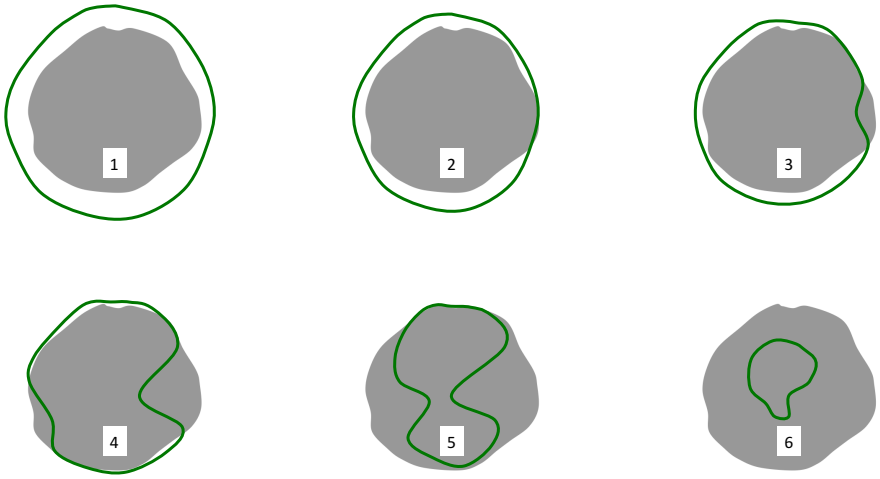

Figure 8: Top-down view showing the typical evolution of the ridge line as an asteroid is spun-up (increasing from 1 to 6) – central zh^* structure not shown for clarity.

rapidly. This can be understood easily when one observes that the gradient of gravity is now much different: outside a body, going towards the center means higher gravity, whereas inside the body, going towards the centre means lower gravity. So the balance between gravity and centrifugal force leads the ridge line to quickly dive inward as soon as a point enters the body. An ever growing section of the ridge line comes inside the body. Eventually, this section of the ridge line reaches the center – or more accurately, merges with the inner zh^* structure. Before that happens, generally, other sections of the ridge line will have entered the body: usually the side opposite to this first section enters the body second. Eventually the ridge line is entirely within the body and continues to shrink towards and with the central structure. Once this situation is obtained, the picture will not change qualitatively anymore, even for arbitrary large spin rates: zh^* will simply continue to shrink around the z-axis.

Of course, what can be seen with the ridge line occurs with the whole h^* outer shell. Hence, at some spin rates, the h^* outer shell carves out whole portions of the body that are not attracted enough to the body to stay in place solely from gravity. The examination of the h^* surface and of sections of the body located beyond it allow to consider possible mechanisms for the fission of the body.

Figure 8 shows a schematic illustration of the behavior of the ridge line based on examples such as 1999 KW4 Alpha, Bennu or 1996 FG3 Alpha. Step 1 is the situation of most asteroids, i.e. slow rotation where the surface is experiencing a downward pull. Step 2 shows the ridge line touching the asteroid at a single point. Step 3 shows the ridge line (and h^* in the 3 dimensions) diving quickly inside the asteroid. In Step 4, h^* has also entered the body on the other side, as it is commonly seen in practice. In Step 5, most of the body is in tension and the two lobes formed by the remnant of the ridge line will soon quickly dive inward as well. Step 6 shows the final qualitative state of this analysis, where the ridge line keeps receding from the surface – in practice it is quickly drawn very close to the pole so that it is barely visible anymore.

3.4. The dynamical conditions allowing fission

Step 2 (see fig. 8) defines the critical spin rate ω_1. At this spin rate, h^* makes first contact with the surface of the asteroid. For our purpose, we are especially interested in steps 2 to 4, where a clearly identified region of the body lies beyond h^*. We can normalize the spin rate of the body by ω_1. It is often found that the ridge line collapses for another critical spin rate, named ω_2, typically not exceeding $1.20\,\omega_1$ (step 5-6 in fig. 8) though the precise value depends on the specific shape of the body. Moreover distinct lobes in the ridge line, such as shown on step 5 (see fig. 8) can be maintained at higher spin rates. Still, we are here examining what happens within a rather narrow range of spin rates, between ω_1 and ω_2, i.e. between 1 and $\approx$1.20 in normalized units.

At such a spin rate, the situation is such that a region of the body is dynamically located outside of the body. Not only does it feel an outward pull, but it also belongs to the outer realm of the body in terms of energy [20, 19]. Indeed, looking at the (conserved) energy of the system, also called Jacobi integral, a portion of the pulled-out region is separated from the rest of the body by a barrier of energy. All the particles forming this region have less energy than required to penetrate inward and have the energy to migrate to infinity. These are the dynamical conditions for fission when considering only centrifugal and gravitational forces.

A particle within such region would be shed as long as it does not hold on to the rest of the asteroids through cohesive forces. The evolution of spin in an asteroid is gradual. As the h^* line dips deeper into the body the centrifugal force acting on the region grows due to both increasing mass and

increasing distance to h^*. When such a pull exceeds the tensile strength that prevents a given particle or aggregate of particles to leave the body, then a whole chunk of the asteroid can break off from the main structure.

4. Fission scenarios

Given the reconstructed parent bodies, we compute, in practice, the dynamical structures presented in the previous section. We then verify whether or not the fission hypothesis works for each body.

4.1. Computation of the ejecta

To see how a body possibly underwent fission, we conduct a survey of the dynamical situation of the body for a range of spin rates. First, we identify the interesting range of spin rates by computing the evolution of the ridge line over a wide range of spin rates. It allows us to identify two values of spin: ω_1, where the ridge line first touches the body, and ω_2, where the ridge line joins the center and disappears. As expected, even for 0 height of the protrusion, the ridge line enters through the protrusion region first. This fact is in itself an interesting preliminary validation of the fission hypothesis for the creation of the cavity: mass placed in the cavity is indeed feeling an outward pull at high spin rates, and nowhere else on the asteroid is this the case.

Yet, the ridge line is only a 1-dimensional object. After it has given us the interesting range of spin rates, for a relatively low computational cost, we compute the h^* surface to obtain the whole picture of the possible fission. In practice, we compute the subset of the h^* surface located at the cavity. To do so, we compute the radius for each point of the cavity/protrusion such that the acceleration on $\hat{\boldsymbol{h}}$ cancels out. In other words, we find h^* by projecting the points of the protrusion onto it.

When h^* carves out a portion of the asteroid, there is a possibility of fission, both dynamically and energetically. It should be noted, first, that the ejecta does not need to be exactly this portion. Indeed, the ejecta could be larger: as long as its center of mass is beyond h^*, its fission is possible. The ejecta could also be smaller, especially when small scale variations of cohesion are present as they could make the triggering of the actual fission quite complex. And generally, the ejecta could simply be different from the pulled region. Figure 9 presents these different possible cases.

In the absence of evidence pointing to a specific option, we chose to compute the fission region with two simple methods. The first method consists in assuming the fission region is equal to the pulled region, carved out by h^*. The second method consists in fixing the fission region to the cavity region, corresponding to the current asteroid shape. In both cases, once this

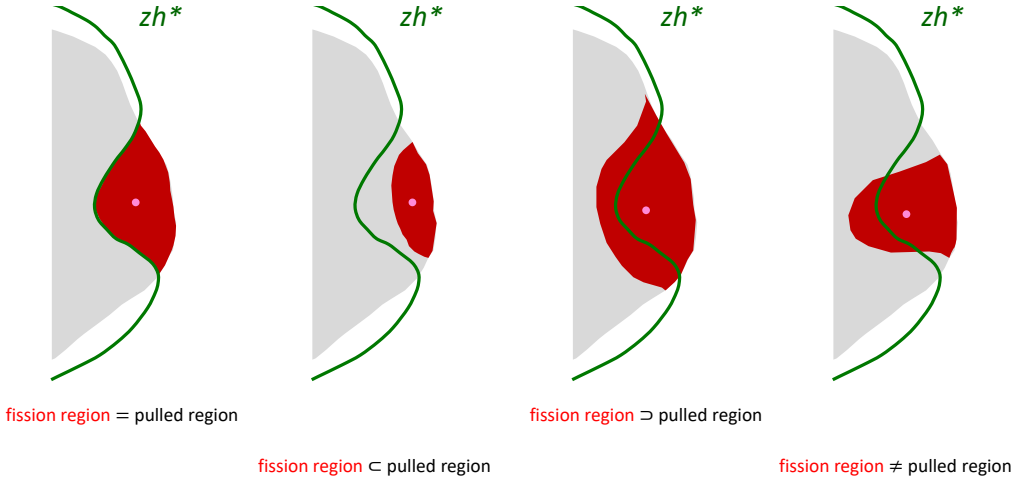

Figure 9: Top-down view showing different fission scenarios, varying the fission region compared to the location of h^*

potential ejecta is obtained, we can compute all of its mass and its center of mass. From these two parameters, we can compute, in a simplified fashion, the total acceleration acting on the ejecta. Computing the inner surface of ejecta, with which it holds on to the rest of the body, we can compute the average stress at this surface.

Note that the computations can be readily adapted to different densities. The balance between gravity potential and centrifugal potential is achieved for a specific ratio of σ/ω^2 (i.e. density over square of the spin rate). If one wants to change the density by a factor f, one can alter the obtained fission spin rate by a factor $\sqrt{f}$ and divide the fission period by $\sqrt{f}$. The stress at the interface should then be multiplied by the same factor f.

4.2. First case: ejecta carved out by h^*

In this case, the mass of the ejecta increases with spin, since the fission region is defined through h^*. The added mass of the protrusion (or simply of the filling of the cavity) allows us to select the fission period corresponding to this scenario: when the mass of the ejecta equals the added mass. This simple assumption considers that no (or only negligible) mass re-impacted the main body after the fission event.

With this fission assumptions, we can present the following fission scenarios. For EV5 and DP107, the results are tabulated in, respectively, table 2

and table 3. In these tables, we give the case's protrusion height, the added mass as a percentage of the mass of the current asteroid, the stress at the interface at the moment of posited fission event, the period of rotation of the body for the posited fission event.

Table 2: Partial fission event of asteroid 2008 EV5

Protrusion height (m)	Added mass (%)	ω_1 period (h)	Fission period (h)	Fission spin (norm. by ω_1)	Interface stress (Pa)
0	0.26	3.20	3.09	1.04	0.02
15	1.22	3.28	3.11	1.05	0.05
30	2.24	3.42	3.14	1.09	0.19
45	3.30	3.57	3.17	1.13	0.38
60	4.42	3.70	3.20	1.16	0.57

Table 3: Partial fission event of asteroid 2000 DP107 Alpha

Protrusion height (m)	Added mass (%)	ω_1 period (h)	Fission period (h)	Fission spin (norm. by ω_1)	Interface stress (Pa)
0	1.65	3.23	3.08	1.05	0.07
30	2.51	3.29	3.10	1.06	0.56
60	3.42	3.42	3.12	1.10	1.3
90	4.36	3.55	3.14	1.13	2.3
120	5.34	3.68	3.17	1.16	3.3

In these fission scenarios, The period of fission is observed to increase as the protrusion mass is increased as well. This effect comes from the observed fact that zh^* is not strongly influenced by the added mass until it touches the surface. Since the protrusion extends further (even despite the recentering of the body) however, h^* touches it sooner. It then dives quickly within the body and reaches the critical mass at a lesser spin rate. Yet, notice that the spin rate, expressed in normalized units of ω_1 (the spin rate where h^* touches the surface), actually increases with the size of the protrusion, as h^* needs to dip further in the body as the added mass increases.

Then, one will note that the added mass typically falls in the range of mass ratio observed for binary systems. Even more interesting, 2000 DP107 is a binary system [6] with a mass ratio of approximately 3.6% which corresponds almost exactly to the 60 m protrusion case. Yet there is no reason to think

that the fission event expelled mass that corresponds exactly to the mass of the *current* secondary: nothing indicates the ejected matter must have remained clustered together as we will discuss later. In any case, we note that the 60 m protrusion case may be especially relevant to the specific story of this binary system.

The shape of the ejecta, at fission, depends on the protrusion height. In fact, low protrusion height show a very narrow ejecta, exhibiting very low radial dive and present on 30-40° longitude wide. Although fission of such a region is possible, it would not create the cavity we observe on 2008 EV5 or 2000 DP107 Alpha. But the ejecta quickly becomes rounder as the added protrusion becomes more massive. However, at its interface with the rest of the body, defined by the shape of h^* per assumption, the ejecta remains flat. This is relevant information as it indicates that, at least macroscopically, most of the stress required to hold the ejecta in place is normal to the interface.

The stress logically increases with the mass of the protrusion. It is also dependent on the mass of the body itself, and not simply its density. This is straightforward to understand when we remember that the stress is computed by dividing the outward force, which is proportional to the volume of the ejecta, by the interface, which is proportional to the surface of the ejecta. The bigger the ejecta, the higher the stress is, all other things being equal.

This computed stress must be understood as both the minimum (macroscopic) tensile strength necessary for the body to have held together up to this spin rate, and also the minimum stress necessary for the chunk to be separated at this instant. If we consider that the macroscopic tensile strength of the chunk is due only to the cohesive forces between its constitutive particles, then this fission hypothesis requires the tensile strength of asteroids to be in the 0.1-10 Pa range. Note here the significant importance of the fission scenario chosen, established with fig. 9. If the fission region is made smaller than the pulled region delimited by h^*, the stress can reach much larger values. Conversely, if the fission region was much smaller, the stress could be even lower. We can examine this effect with the second fission case, where the fission region is fixed a priori.

4.3. Second case: ejecta fixed by current shape

In this case, the current shape of the asteroid allows us to predetermine an ejecta. The shape of the ejecta can be initially computed by joining the current cavity area shape with the assumed parent protrusion area shape.

The current cavity area is the interface of the ejecta with the parent body, while the assumed protrusion area is the exterior surface. Joined together, they form a chunk that if ejected whole from the parent body would exactly recreate the present shape.

But this simplistic model must be amended as this chunk shape makes it very unlikely to be coherent: it exhibits thin extensions at high latitudes. This extensions most likely resurfaced the cavity at the moment of fission. In practice, computing fission with these extensions yields to underestimating the stress for two main reasons: 1. it pushes the center of gravity of the chunk inward 2. it significantly increase the area of the interface. Thus we eliminate these extensions from the fission region. To compensate for the (small) mass they were contributing, we push the interface surface slightly inward (a few meters at most). In the end, the mass of the fission region is equal to the added mass, hence creating a suitable fission case.

Contrarily to the first fission case considered, we do not have a way to pinpoint a specific fission period, as the fission mass always equals the added mass. There is a maximum spin period, where h^* reaches the center of gravity of the ejecta and the outward force and stress are infinitesimal. Below this maximum spin period, the interface stress varies since the outward force will increase with the spin rate. In fact, increasing the spin rate can make the interface stress as large as desired. And no matter how high the spin rate is, the protrusion region will always be experiencing the largest outward force. The stress was computed for rotation period between 2.5 h and 3.5 h. At 2.5 h, for all the protrusion scenarios considered, the whole equator was in tension, hence making it an upper bound of the fission period. As the fission mechanism would probably induce a small shock into the whole body that could counter the weak tensile strength, an equator in tension would probably be entirely set loose at the moment of fission. It is therefore considered that 2.5 h is our lower bound for the period of fission.

Figure 10 shows the evolution of the stress as a function of the normalized spin rate ω/ω_1 (left) and the rotation period (right) for 2008 EV5. Figure 11 shows this evolution for 2000 DP107. Note that all curves reach zero stress when h^* reaches the center of gravity of the ejecta. All figures display the evolution from a rotation period between 2.5 h and 3.5 h, and the normalized spin rate curves right end correspond to this 2.5 h limit.

In this second case, higher tensile strength values are possible than for the first case. That being said, the highest values displayed, about 4 Pa for 2008 EV5 and 25 Pa for 2000 DP107 since these values are attained for very high

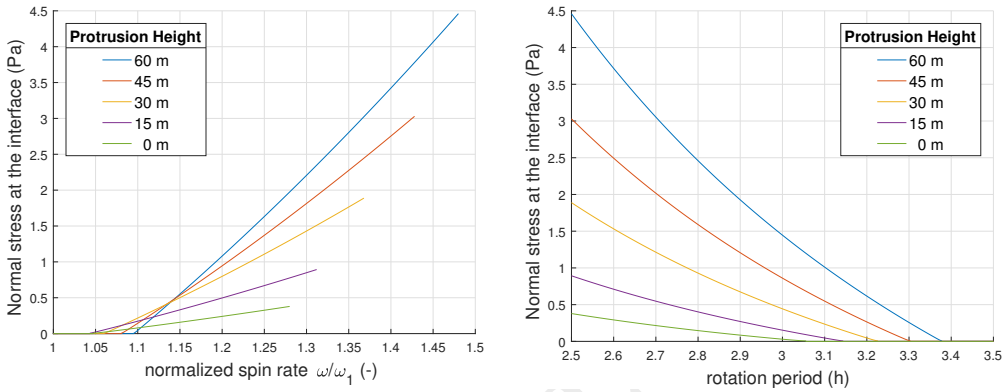

Figure 10: Stress at the ejecta interface as a function of normalized spin rate (left) and period (right) for 2008 EV5.

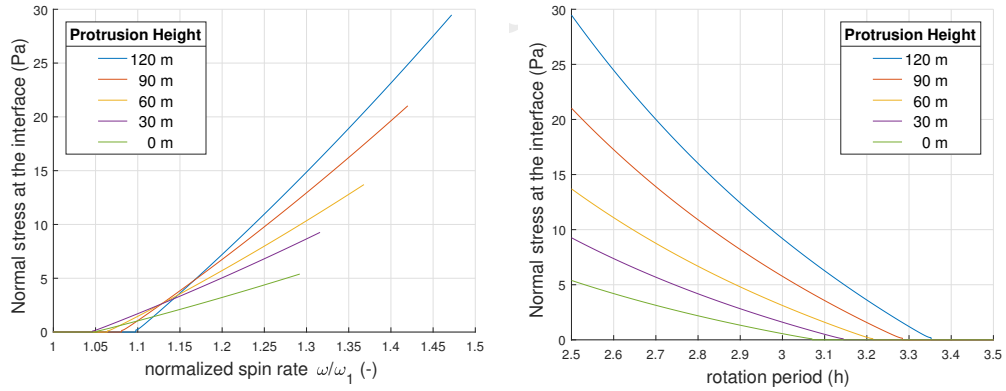

Figure 11: Stress at the ejecta interface as a function of normalized spin rate (left) and period (right) for 2000 DP107.

values of the normalized spin rate. As aforesaid, at these levels, the whole equator is in tension: a fission would likely set a chain reaction that would let loose the whole equatorial ridge. Nevertheless, we can say with these results that the previous section depicted low values of the tensile strengh for the fission mechanism. The range for 2008 EV5 could have reached up to 2 Pa, while for 2000 DP107 it could have reached up to 15 Pa.

Nevertheless, the values obtained still contrast with the currently estimated cohesion of asteroid material, especially the low value for 2008 EV5. It is estimated that the tensile strength ranges around 50-250 Pa [21, 22]. This is about 1 to 2 order of magnitudes above what this fission mechanism requires. This discrepancy could point to a simple need to restrict the fission region and in turn see fission occur for higher spin rates. But other explanations are possible and that is what the final section of this paper will present.

4.4. The fate of the ejecta

However, before going to the investigation of the cohesion, consider the likely fate of ejecta separated from the surface. There are a range of possible morphologies for this ejected material, ranging from a single monolithic boulder to a collection of finer regolith held together with a slightly stronger degree of cohesion. For definiteness, we will assume that the separated material remains coherent.

If we assume the ejecta remains for the most part intact, we can define its initial orbit. Because the spin rate remains relatively slow at the moment of fission, the ejecta is placed on a tight elliptical orbit whose (instantaneous) periapse is at the fission location (in inertial space). Yet, because this orbit is very close to the primary body, massive perturbations should be expected on this first arc. The astrodynamics of this problem are really of the full-body type [23], rather than the point mass (i.e. restricted) type; nevertheless, treating the ejecta as a point mass, it does not have the energy to reimpact the body anywhere, but only close to the cavity and sometimes on the other side as well, where potential is also low. This first orbital arc could lead the ejecta to reimpact at low speed. But it could also lead the ejecta to gain in semi-major axis and reduce its eccentricity. From there on, complex orbit-spin coupling dynamics would decide the ultimate fate of the ejecta. The timescale of this regularization remains much lower than that of YORP effects and can lead to binary systems that are stable at YORP time scales [9, 23, 24, 25].

2000 DP107 Alpha has a companion: it would be an example of the stable (or recent) binary system. But 2008 EV5 is, as far as we know, a single asteroid: the fissioned material either escaped from the system or redeposited at the surface. In the case of an escaped secondary, we find in practice a quasi-linear relationship between the mass ratio secondary/primary and the variation of spin rate that results from the loss of momentum. Indeed, for every 2% mass fissioned and escaped, about 3% spin rate is lost. For example, for the protrusion height of 60 m, the spin rate of EV5 should have decreased by almost 7%. For the 30 m protrusion heigh, the spin rate would only have decreased of about 3.5%. But these calculations assume notably that the whole secondary is ejected, which is far from certain. In any case, the spin rate variation still remains inferior to 10%: it keeps the asteroid spinning at a very fast rate (above the ω_1 value computed for the parent body). Yet, the mass distribution has changed, hence the h^* surface does not necessarily enter the body anymore. Note that the variation of the spin rate is not influenced by the change of density, as long as the asteroid remains homogeneous.

5. The structure of fast spinning asteroids

We have established a mechanism for fission of a fast spinning small body. Through the complex balance of centrifugal and gravitational force, a chunk can be ejected at moderately high spin rate while the rest of the body experiences no or minimal effects from this too large spin rate. Yet, for our explanation to hold, the value of tensile strength at the interface between the ejected chunk and the remaining body must be around 1 Pa. As aforesaid, this is a low value and it can contrast with many other, higher estimations. Although the spin barrier observed on small bodies can be obtained with these low strength values, this could be a real discrepancy of our research. But there are many possible explanations to this potential discrepancy.

A possible explanation is that 2008 EV5 and 2000 DP107 Alpha are unusual asteroids and happen to have very low cohesion. Another is that, even though their global cohesion is normal, they exhibited very low cohesion at the location of the protrusion (now cavity) by simple chance. These kind of explanations have the problem that they are entirely unfalsifiable, and give almost no predicting capabilities.

Another range of explanation consists in looking into the actual estimation of asteroid cohesion. Only two asteroids have been observed to undergo fission, hardly a statistical sample. Some asteroids have been observed intact despite an outward stress up to 200 Pa, but that could just be the result of a survivor bias: we cannot observe the ones that did not survive. The problem of this explanation is that it may be a long time before we can observe statistically enough fissions to establish the experimental range of cohesion: it pushes back the verification too far in the future to be of any interest today.

There is a last explanation possible: the low cohesion observed is caused by the specific evolution of the asteroid. We think that the cohesion at the equator of 2008 EV5, 2000 DP107 and possibly other bicone asteroids is much smaller than both elsewhere on the asteroid and on other asteroids because of the very processes that led to the formation of the bicone shape. As we will see, this explanation is readily verifiable/falsifiable and in line with current observations. This section develops and explains this justification.

5.1. Strong cores

The usual approach to the study of granular asteroids, be this through Soil Mechanics Theory or computer simulations, has been to assume that their interiors are homogeneous; however, this does not need to be so. A

look at the pictures of the surfaces of the different asteroids that have been visited show surfaces covered with grains with a size distribution that goes from micrometers to decameters. If we take the morphology of the surface as a reflexion of the interior, this should lead us to see that interiors could be heterogeneous in porosity, bulk density or strength among other characteristics.

As it is explained in [17], an aggregate with homogeneous cohesion would always fail internally before it fails superficially. This process would produce a bicone asteroid as the poles push inward and a broken interior pushes outward [26], leaving a somewhat intact surface. However, if the core is strengthened and is able to withstand the otherwise, high rotational rates, the aggregate would fail at the surface first, provoking severe surface flow towards the equator. This specific internal structure and failure mode would also generate a bicone aggregate though somewhat asymmetric as it would have a protrusion on one side. This process has been presented in Sánchez et al. [18] and we reproduce in fig. 12 the typical deformation that can be obtained with a strong core, showing a very large protrusion on one side.

We will not try to explain how a given asteroid could have acquired a strong interior as that is beyond the focus of this paper. However, it should be established that this can be acquired due to a number of factors: higher density material, stronger cohesive forces between the grains, higher packing fraction, a big central monolith, an icy core, etc., or due to a combination of them.

5.2. Kinetic sieving forming rocky equators

If the above scenario is true, the equatorial ridge would then be formed by the flow of material from the mid-latitudes towards the equatorial region [10] and the protrusion would be formed where the greatest amount of material flowed towards the equator. Now we need to take a closer look at this granular flow and to a process called kinetic sieving.

Kinetic sieving is the dominant mode of segregation in granular avalanches, where separation of particles occurs according to size. Briefly, when a polydisperse mixture of grains flows downslope, the local filling fraction is going to fluctuate and the smaller particles are going to fall through the spaces that open up between the larger grains simply because they are more likely to fit into the available space than the larger ones. The reader is referred to Gray et al. [27] and Savage et al. [28] for an in-depth analysis of the process. In their research, the authors mention that this process is the key

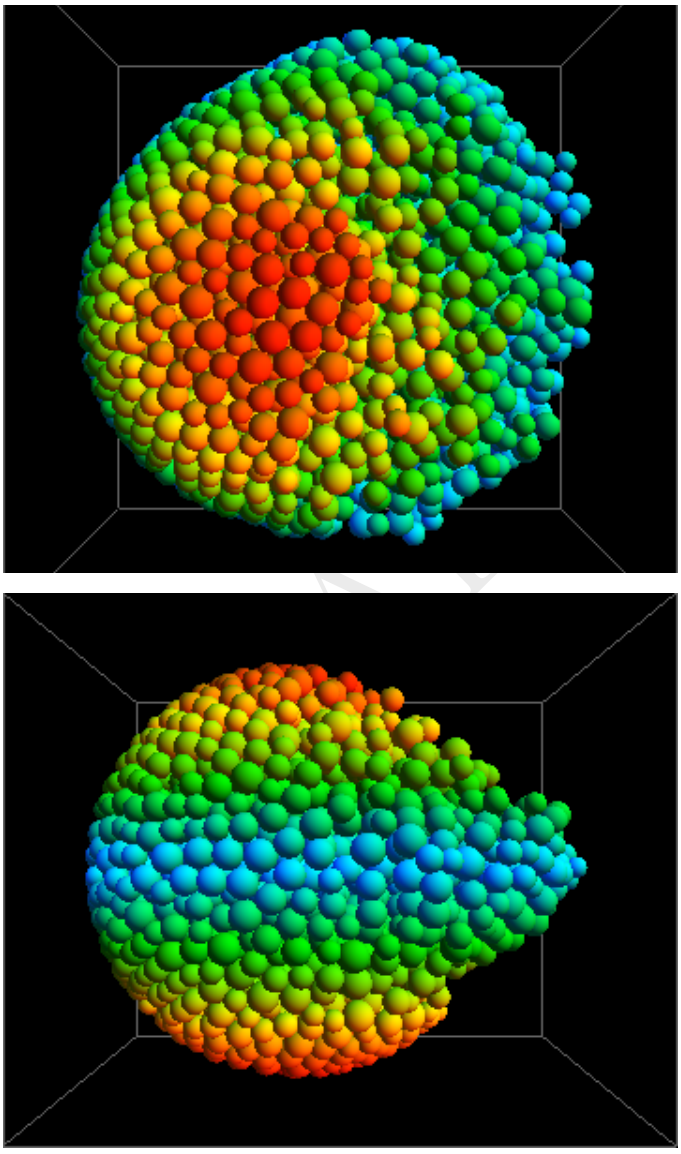

Figure 12: Deformation of an asteroid possessing a strong core, from Sanchez et al. [18], viewed from the top (top) and the side (bottom). It displays a very important and wide protrusion. Colors change with latitude

mechanism for the formation of layers of larger particles overlying layers of fines. In geology, this is known as reverse grading. If an inversely graded layer is sheared, large particles tend to migrate towards the front of the flow and smaller ones towards the rear [29, 27]. Of course, these studies have been carried out for dry, cohesionless granular materials and studies on cohesive grains have introduced cohesive forces through moisture and liquid bridges[30, 31]. In their work, they conclude that particle segregation is indeed reduced for Bond numbers B_0 (ratio of maximum cohesive force to weight of a particle) $\geq$1 as cohesive forces can be strong enough to stop the smaller grains form percolating. In the asteroid environment, and as shown by Scheeres, et al. [32], B_0 of $\approx$1 can be obtained for particles in centimeter size range in the best possible scenario. However, the size distribution that has been measured in asteroid Itokawa goes from microns to tens of meters and for particles with sizes greater than a centimeter, B_0 decreases rapidly. Furthermore, even if the aforementioned studies and conclusions about the segregation of wet cohesive particles can be also applied for dry, cohesive particles as those found in asteroid surfaces, segregation is not fully avoided. Furthermore, perfect segregation is not fully required as it is explained below.

If we apply this idea of kinetic sieving to the granular flows on the surface of an asteroid, we could expect that the same mechanism should have taken place on it. Though the magnitude of ambient gravity can be orders of magnitude smaller than on Earth, it is its existence along with a Bond number less than 1 that warrants that the segregation process can take place. This should then create a size segregated asteroid surface due to granular flows. Under this formation model, the bicone asteroid would have a very rocky equator and more sandy tropics. As it was explained in Sánchez and Scheeres [33], the tensile strength of a cohesive aggregate is directly proportional to the packing fraction (ϕ) and inversely proportional to the average particle radius (see eq. 6 in said paper). A rocky equatorial region would ensure the decrease of the former and the increase of the latter. As such, size segregation would diminish the tensile strength of the equatorial ridge, especially that of the protrusion due to its larger particle composition and greater porosity, making it possible to obtain the low tensile strength that the cavity formation process described in this paper requires.

5.3. Simulations and observations

Simulation showing that a self-gravitating aggregate can be deformed through rotation and form a protrusion have already been carried out by

[34]. Those simulations where carried out with a simulation code that implements a Soft-sphere Discrete Element Method (SSDEM) as is explained in many previous works, notably [35, 33, 18]. The aggregates used implemented also cohesive forces and strong cores, and so we will not repeat them here. However, the particles used in these simulations are too few and have a very narrow size distribution making it impossible to see any kind of segregation.

In order to test the validity of the process described in this paper we have followed the suggestion made by Scheeres[10] and simulated only a small slice of a spherical aggregate whose evolution will be observed. This slice has been stretched out so that in the absence of rotation, the gravity vector is constant and the simulation is carried out in the rotating frame of reference. By doing this we avoid the calculation of self-gravity and are able to increase the number of particles as well as to widen the size distribution. Fig. 13 shows snapshots of the initial, middle and final state of the simulated system showing how the larger particles readily migrate to the equatorial region at high enough rotation rates. In this simulation, the small particles are white, the large ones are red and there is a factor of $\approx$4 difference in their size. The number of large particles is such that their volume is the same as that of the small one. Additionally, the particles at the bottom are stuck to it in order to mimic a strong core and the aggregate as a whole has an angle of friction of $35^\circ - 40^\circ$ as static, dynamic and rolling friction have been implemented.

This simulation shows the possibility of kinetic sieving at the surface of asteroid. We can recreate what the asteroid would look like by bending this slice to its actual shape and replicating it around the pole of the asteroid. Figure 14 is the result we obtain, and where we clearly see both the biconic shape and the roky aspect of the equator. There has not been any observation of this sieving on bicone asteroid yet, since no mission has visited one yet and as the radar modeling does not have the resolution required. However, this process could contribute to lower the thermal inertia of the asteroid, an effect that may be observable. Indeed a rocky equator would present a much lower thermal inertia than the average regolith and would lower the average thermal inertia of the whole asteroid. Interestingly, Delbo et al.[36] have concluded that there may be a noticeable difference in thermal inertia between binaries and single asteroids: binaries would have a higher thermal inertia (making them generally cooler). This observation could be explained by a rocky equator.

OSIRIS-REx will arrive at Bennu in 2018. Bennu is another bicone asteroid, and could have experienced spin-up in its past [20], perhaps up to fission

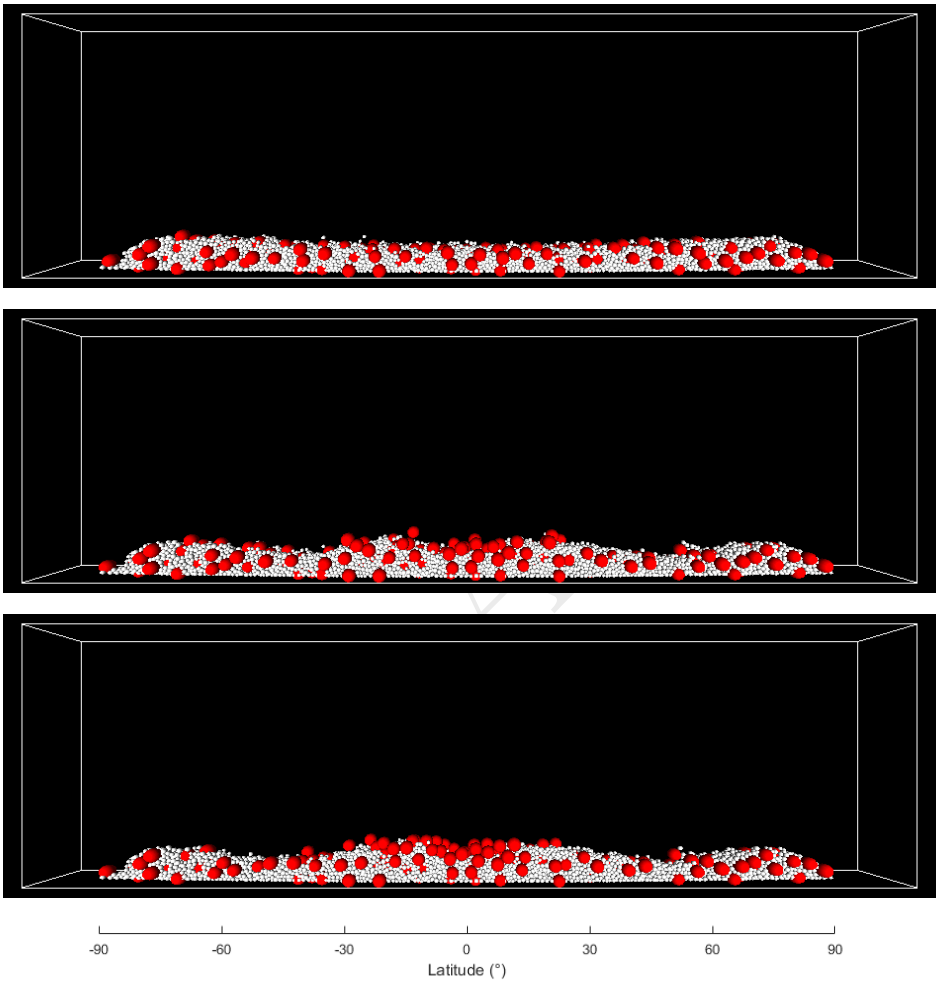

Figure 13: Simulation of a longitudinal slice (lune) of an asteroid surface, composed of a bimodal distribution of large and small particles, undergoing spin-up. Initially, particles are homogeneously partitioned within the slice (top figure). The spin-up brings more material to the equator and progressively segregates the distribution (middle figure). At the end of the process, the equator is of rocky appearance as the rocks have been brought above the sandy material (bottom figure).

Figure 14: Reconstitution of a full asteroid before deformation (top) and after deformation (bottom), from the longitudinal slices shown on Fig 13, seen at an elevation angle of 15°. After deformation, the asteroid shape has become biconic and its equator rocky.

point. The first high-resolution picture of the surface will undoubtedly shed light on the behavior of regolith at the surface of bicones. If the equator is visibly rocky, it would confirm our assumptions and the proposed mechanisms. On the other hand, the formation of bicones is not fully understood. A different observation could point us to different explanations, either linked to the specific history of Bennu or to more general aspects of bicone asteroids, and among other things: presence or absence of core, of large boulders, or of kinetic sieving and Brazil-nut effects.

6. Conclusions

In this paper we take a close look at a possible formation mechanism of the equatorial cavities that asteroids 2008 EV5 and 2000 DP107. We hypothesize that both cavities could be the result of rotational fission driven by the YORP effect and that in both cases, the cavities were formed by the ejection of a coherent piece of the original asteroids. This hypothesis is not only an explanation for the existence of the cavities but also describes a plausible mechanism for binary formation.

For our analysis we calculate the geometrical locus of the points at which centrifugal and gravitational forces balance and find that, if these asteroids were to have a filled cavity or a protrusion in its place, this surface (the ridge line in 2D) would enter the asteroids exactly where the cavity has formed. Taking this as a starting point, we calculate the needed cohesive strength that the surface of the asteroids should have in order to eject a complete, coherent piece as large as the cavities themselves. In accordance with our calculations, this strength should be low: between 0 to 2 Pa for 2008 EV5, between 0 to 15 Pa for 2000 DP107. This is 1 to 2 orders of magnitude smaller than the strength measured for the few asteroids which disruption has been observed.

In order to address this discrepancy we argue that, just like on Earth, granular flow of the asteroid surfaces could have driven size segregation of particles through kinetic sieving. Surface flows can occur in asteroids as long as they have an interior (core) that is structurally stronger than the outer surface (shell) as otherwise the interior will fail first at high enough rotation rates. Rotation would drive granular flow from the mid latitudes towards the equatorial region, helping with the formation of the equatorial ridge and kinetic sieving would ensure that this ridge is formed by the larger particles in the flow. In turn larger particles will form a less cohesive, more porous medium that could easily reach the low values for tensile strength that this fission and binary formation mechanism requires.

Observations of asteroids could shed light on this hypothesis. A more rocky equator may be detectable from ground-based observations if it affects the properties of bicones significantly. The arrival of OSIRIS-REx at Bennu in 2018 will be a major milestone for understanding the mechanisms and properties of bicone asteroids as Bennu. It may confirm our hypothesis or direct us to revisit some aspects of this study.

7. Acknowledgments

The authors would like to acknowledge Dr. Michael Busch for this suggestions and comments, notably for highlighting the case of 2000 DP107. The authors give thanks to Dr. Shantanu Naidu for providing a high resolution shape model of 2000 DP107. The authors also thank Dr. William Bottke for an insightful correspondence pertaining to asteroid-asteroid collisions and impact cratering. Finally, the authors greatly appreciated the inputs of Dr. Masatoshi Hirabayashi, on the role of cohesion in the fission mechanism presented here.

Daniel J. Scheeres and Paul Sánchez acknowledge support of grants from NASA's NEOO program (NNX14AL16G) and from the SSERVI program.

[1] J. Miller, A. Konopliv, P. Antreasian, J. Bordi, S. Chesley, C. Helfrich, W. Owen, T. Wang, B. Williams, D. Yeomans, et al., Determination of shape, gravity, and rotational state of asteroid 433 eros, Icarus 155 (1) (2002) 3–17.

[2] A. Fujiwara, J. Kawaguchi, D. K. Yeomans, M. Abe, T. Mukai, T. Okada, J. Saito, H. Yano, M. Yoshikawa, D. J. Scheeres, O. Barnouin-Jha, A. F. Cheng, H. Demura, R. W. Gaskell, N. Hirata, H. Ikeda, T. Kominato, H. Miyamoto, A. M. Nakamura, R. Nakamura, S. Sasaki, K. Uesugi, The rubble-pile asteroid itokawa as observed by hayabusa, Science 312 (5778) (2006) 1330–1334.

[3] H. Yano, T. Kubota, H. Miyamoto, T. Okada, D. Scheeres, Y. Takagi, K. Yoshida, M. Abe, S. Abe, O. Barnouin-Jha, A. Fujiwara, S. Hasegawa, T. Hashimoto, M. Ishiguro, M. Kato, J. Kawaguchi, T. Mukai, J. Saito, S. Sasaki, M. Yoshikawa, Touchdown of the hayabusa spacecraft at the muses sea on itokawa, Science 312 (5778) (2006) 1350–1353. arXiv:http://www.sciencemag.org/content/312/5778/1350.full.pdf, doi:10.1126/science.1126164.
URL http://www.sciencemag.org/content/312/5778/1350.abstract

[4] F. Preusker, F. Scholten, K.-D. Matz, T. Roatsch, K. Willner, S. Hviid, J. Knollenberg, L. Jorda, P. J. Gutiérrez, E. Kührt, et al., Shape model, reference system definition, and cartographic mapping standards for comet 67p/churyumov-gerasimenko–stereo-photogrammetric analysis of rosetta/osiris image data, Astronomy & Astrophysics 583 (2015) A33.

[5] M. W. Busch, S. J. Ostro, L. A. M. Benner, M. Brozovic, J. D. Giorgini, J. Jao, D. J. Scheeres, C. Magri, M. C. Nolan, E. S. Howell, P. A. Taylor, J. L. Margot, Brisken, Radar observations and the shape near-earth asteroid 2008 ev5, Icarus 212.

[6] S. P. Naidu, J.-L. Margot, P. A. Taylor, M. C. Nolan, M. W. Busch, L. A. Benner, M. Brozovic, J. D. Giorgini, J. S. Jao, C. Magri, Radar imaging and characterization of the binary near-earth asteroid (185851) 2000 dp107, The Astronomical Journal 150 (2) (2015) 54.

[7] K. J. Walsh, D. C. Richardson, P. Michel, Rotational breakup as the origin of small binary asteroids, Nature 454 (2008) 188–191.

[8] J. L. Margot, M. C. Nolan, L. A. M. Benner, S. J. Ostro, R. F. Jurgens, J. D. Giorgini, M. A. Slade, D. B. Campbell, Binary asteroids in the near-earth object population, Science 296 (5572) (2002) 1445 – 1448.

[9] S. A. Jacobson, D. J. Scheeres, Dynamics of rotationally fissioned asteroids: Source of observed small asteroid systems, Icarus 214 (1) (2011) 161 – 178.

[10] D. Scheeres, Landslides and mass shedding on spinning spheroidal asteroids, Icarus 247 (0) (2015) 1 – 17. doi:http://dx.doi.org/10.1016/j.icarus.2014.09.017.
URL http://www.sciencedirect.com/science/article/pii/S0019103514004795

[11] M. K. Shepard, J.-L. Margot, C. Magri, M. C. Nolan, J. Schlieder, B. Estes, S. J. Bus, E. L. Volquardsen, A. S. Rivkin, L. A. Benner, et al., Radar and infrared observations of binary near-earth asteroid 2002 ce26, Icarus 184 (1) (2006) 198–210.

[12] M. C. Nolan, E. Asphaug, H. J. Melosh, R. Greenberg, Impact craters on asteroids: Does gravity or strength control their size?, Icarus 124 (2) (1996) 359–371.

[13] W. F. Bottke, D. D. Durda, D. Nesvornỳ, R. Jedicke, A. Morbidelli, D. Vokrouhlickỳ, H. F. Levison, Linking the collisional history of the main asteroid belt to its dynamical excitation and depletion, Icarus 179 (1) (2005) 63–94.

[14] W. Bottke, M. C. Nolan, R. Greenberg, R. A. Kolvoord, Collisional lifetimes and impact statistics of near-earth asteroids, Hazards due to comets and asteroids 337.

[15] K. A. Holsapple, On yorp-induced spin deformations of asteroids, Icarus 205 (2) (2010) 430–442.

[16] D. Jewitt, J. Agarwal, J. Li, H. Weaver, S. Larson, Disintegrating asteroid p/2013 r3, The Astrophysical Journal Letters 784 (1).

[17] M. Hirabayashi, D. J. Scheeres, T. Gabriel, et al., Constraints on the physical properties of main belt comet p/2013 r3 from its breakup event, The Astrophysical Journal Letters 789 (1) (2014) L12.

[18] P. Sánchez, D. J. Scheeres, Disruption patterns of rotating self-gravitating aggregates: A survey on angle of friction and tensile strength, Icarus 271 (2016) 453–471.

[19] S. Tardivel, The deployment of scientific packages to asteroid surfaces, Ph.D. thesis, University of Colorado Boulder (2014).

[20] D. Scheeres, S. Hesar, S. Tardivel, M. Hirabayashi, D. Farnocchia, J. McMahon, S. Chesley, O. Barnouin, R. Binzel, W. Bottke, et al., The geophysical environment of bennu, Icarus 276 (2016) 116–140.

[21] M. Hirabayashi, D. J. Scheeres, Stress and failure analysis of rapidly rotating asteroid (29075) 1950 da, The Astrophysical Journal Letters 798 (1) (2014) L8.

[22] D. Polishook, N. Moskovitz, R. Binzel, B. Burt, F. DeMeo, M. Hinkle, M. Lockhart, M. Mommert, M. Person, A. Thirouin, et al., A 2km-size asteroid challenging the rubble-pile spin barrier–a case for cohesion, Icarus 267 (2016) 243–254.

[23] D. J. Scheeres, et al., Dynamical configuration of binary near-earth asteroid (66391) 1999 kw4, Science 314 (2006) 1280–1283.

[24] D. Scheeres, Stability of binary asteroids, Icarus 159 (2) (2002) 271–283.

[25] S. A. Jacobson, D. J. Scheeres, Long-term stable equilibria for synchronous binary asteroids, The Astrophysical Journal Letters 736 (L19).

[26] M. Hirabayashi, D. J. Scheeres, Stress and failure analysis of rapidly rotating asteroid (29075) 1950 da, The Astrophysical Journal Letters 798 (1) (2015) L8.

[27] J. Gray, A. Thornton, A theory for particle size segregation in shallow granular free-surface flows, in: Proceedings of the Royal Society of London A: Mathematical, Physical and Engineering Sciences, Vol. 461, The Royal Society, 2005, pp. 1447–1473.

[28] S. Savage, C. Lun, Particle size segregation in inclined chute flow of dry cohesionless granular solids, Journal of Fluid Mechanics 189 (1988) 311–335.

[29] N. Thomas, Reverse and intermediate segregation of large beads in dry granular media, Physical Review E 62 (1) (2000) 961.

[30] A. Anand, J. S. Curtis, C. R. Wassgren, B. C. Hancock, W. R. Ketterhagen, Segregation of cohesive granular materials during discharge from a rectangular hopper, Granular Matter 12 (2) (2010) 193–200.

[31] H. Li, J. McCarthy, Controlling cohesive particle mixing and segregation, Physical review letters 90 (18) (2003) 184301.

[32] D. Scheeres, C. Hartzell, P. Sánchez, M. Swift, Scaling forces to asteroid surfaces: The role of cohesion, Icarus 210 (2) (2010) 968–984.

[33] P. Sánchez, D. J. Scheeres, The strength of regolith and rubble pile asteroids, Meteoritics & Planetary Science 49 (5) (2014) 788–811.

[34] M. Hirabayashi, D. P. Sánchez, D. J. Scheeres, Internal structure of asteroids having surface shedding due to rotational instability, The Astrophysical Journal 808 (1) (2015) 63.

[35] P. Sánchez, D. J. Scheeres, Simulating asteroid rubble piles with a self-gravitating soft-sphere distinct element method model, The Astrophysical Journal 727 (2).

[36] M. Delbo, K. Walsh, M. Mueller, A. W. Harris, E. S. Howell, The cool surfaces of binary near-earth asteroids, Icarus 212 (1) (2011) 138–148.